Draft of changes 8/9/93

RADIO EMISSION FROM THE HELIOPAUSE TRIGGERED BY AN INTERPLANETARY SHOCK

by

D. A. Gurnett[1], W. S. Kurth[1],
S. C. Allendorf[1], and R. L. Poynter[2]

August 1993

[1]Department of Physics and Astronomy,
The University of Iowa
Iowa City, Iowa 52242

[2]Jet Propulsion Laboratory,
4800 Oak Grove Drive
Pasadena, California 91109

Submitted for Publication to *Science*

Abstract

A strong new heliospheric radio emission event has been detected by Voyagers 1 and 2 in the frequency range from 2 to 3 kHz. This event started in July, 1992, and is believed to have been generated at or near the heliopause by an interplanetary shock that originated from a period of intense solar activity in late May and early June, 1991. This shock produced large plasma disturbances and cosmic ray intensity decreases at Earth, Pioneers 10 and 11, and Voyagers 1 and 2. The average propagation speed estimated from these effects is 600 to 800 kilometers per second. After correcting for the expected decrease in the shock speed in the outer heliosphere, the distance to the heliopause can be estimated, and is in the range from 116 to 177 Astronomical Units.

INTRODUCTION

The heliopause is the boundary between a hot ($\sim 10^5$ K) ionized gas flowing outward from the Sun called the solar wind (1), and the interstellar medium, which is a relatively cool ($\sim 10^4$ K) partially ionized gas between the stars. Since the Sun is moving with respect to the nearby interstellar medium, the heliopause is expected to form a teardrop-shaped surface, the nose of which is toward the direction of the arrival of the interstellar gas (2). The region inside the heliopause is called the heliosphere. Estimates of the distance to the heliopause based on our limited knowledge of the interstellar medium have varied from a few tens of AU (astronomical unit, 1.49×10^8 km) to several hundred AU. For a recent review of the heliosphere and its interaction with the interstellar medium see Suess (3). Four spacecraft, Pioneers 10 and 11, and Voyagers 1 and 2, are on escape trajectories from the Sun to study the outer heliosphere and to penetrate into the interstellar medium. None has yet reached the heliopause, or the solar wind terminal shock, which is a standing shock that is expected to form in the supersonic solar wind flow well inside of the heliopause. The radio emissions described in this report and their interpretation have the potential of providing the first direct measurement of the distance to the heliopause.

DESCRIPTION OF THE EVENT

Frequency-time spectrograms of the new radio emission event are shown in Figure 1. The top panel is from Voyager 1, which was located at a heliocentric radial distance of R = 50.8 AU, and a solar ecliptic latitude and longitude of β = 33.6° and λ = 245° (as of January 1, 1993), and the bottom panel is from Voyager 2, which was located at R = 39.0 AU, β = -11.7°, and λ = 283°. These spectrograms were obtained from the wideband plasma wave receiver, which provides periodic samples of the electric field waveform over a bandwidth of 50 Hz to 10 kHz. For a description of the Voyager plasma wave instrument (PWS) see Scarf and Gurnett (4). The spectrograms cover a frequency range from 1 to 4 kHz, and a time span of one year, from day 120, 1992, to day 120, 1993. The electric field intensity at any given frequency and time is indicated by the color, with red being the most intense and blue being the least intense.

Two primary spectral components can be seen in Figure 1: a main band at about 2.0 kHz, and a series of narrowband emissions drifting upward in frequency at a rate of about 2.8 kHz/year, reaching a peak frequency of about 3.6 kHz. The main emission band has a sharply defined low frequency cutoff at 1,8 kHz. The emissions consist of electromagnetic waves since they occur at frequencies well above the local plasma frequency. The plasma frequency (f_p = 9000$\sqrt{N}$ Hz, where N is the electron density in cm^{-3}) is the low frequency cutoff of free space electromagnetic waves, and corresponds approximately to the high frequency limit of locally generated plasma waves. For the time period of interest the plasma frequency, as determined by the Voyager 2 plasma instrument, ranges from 0.4 to 1.3 kHz, with a mean of around 0.7 kHz (s). The exact starting time of the radio emission is difficult to determine from the wideband data, since the time resolution early in the event is only one spectrum per week. The sampling

times are indicated by the short vertical bars at the tops of the spectrograms. A more accurate starting time can be obtained from the PWS 16-channel spectrum analyzer data, which provides one measurement every 16 seconds. The 16-channel spectrum analyzer data show that the radio emission first appeared in the 1.78 kHz channel on day 188 (July 6), 1993. After the start of the event the intensity gradually increased over a period of months, reaching a peak in early December 1992. Thereafter, the intensity gradually decreased and is almost down to the receiver noise level, as of July 1993.

A striking characteristic of the overall event is the close similarity of the spectrums at the two spacecraft, even though they are separated by a distance of 44.6 AU. This close similarity suggests that the source is at a considerable distance, more than 44 AU. From the maximum radiation intensity (1.8×10^{-17} Watts $m^{-2}Hz^{-1}$) the radiated power is estimated to be at least 10^{13} Watts. This radio source is much stronger than any known planetary radio emission, and is probably the most intense radio source in the solar system.

Radio Direction Finding Measurements

Voyager is normally stabilized in a fixed inertial orientation with the high gain antenna pointed toward the Earth. However, once every three months the spacecraft performs a series of rolls around the high gain antenna axis to calibrate the magnetometer. Three such roll maneuvers were performed during this event, the first two on days 220 and 311 of 1992, and the third on day 36 of 1993. Since the PWS dipole antenna axis is perpendicular to the roll axis, these maneuvers can be used to perform radio direction finding measurements. The 16-channel spectrum analyzer data must be used for these measurements since the sample rate of the wideband spectrum is too low to resolve the roll modulation.

Also, because of a data system failure on Voyager 2 shortly after launch, direction finding measurements can only be performed on Voyager 1.

(My two spectrum analyzer channels, 1.78 and 3.11 kHz, are in the proper frequency range to detect the heliospheric radio emission. Of these, no roll-modulation effects were observed in the 1.78 kHz channel. However, a clear roll-modulation signal was observed in the 3.11 kHz channel during all three maneuvers. An example of this roll modulation is shown in Figure 2, which is for a ten turn roll maneuver on day 220. The sinusoidal modulation in the electric field intensity at twice the rotation period of the spacecraft is clearly evident. '1'0 determine the amplitude and phase of the modulation a sine function was fit to the. data using a least squares fitting procedure. The best fit is shown by the smooth curve. All three roll maneuvers had similar modulation signatures. The peak-to-peak modulation amplitudes range from shout 10 to 20 percent. These relatively low modulation amplitudes indicate that the source is either relatively large (> 60°), or that the source is located well away from the Ion axis (-- 400), or a combination of these effects. The existence of a significant anisotropy also indicates that the radiation (at 3.11 kHz) is not trapped in a high-Q cavity as suggested by Czechowski and Grzedzielski (6). Multiple reflections in a cavity would be expected to quickly lead to anisotropic electric field distribution.

For a rotating. electric dipole, it can be shown that the source must lie. in a plane perpendicular to the. antenna axis at the time of maximum signal strength (i. e., from the phase of the roll modulation). If the antenna axis is perpendicular to the roll axis, as it is during these maneuvers, then the plane through the source also contains the 1011 axis. "1'0 visualize possible source locations, it is convenient to construct a diagram looking along the roll axis as in Figure 3, with all vectors projected onto a plane

perpendicular to the roll axis. In this diagram, the plane. through the source reduces to a line with two possible directions, shown by the dashed lines with arrows at either end.

As can be seen from Figure 3, the observed source directions tend to cluster around the projected direction of the Sun's motion. This clustering is consistent with a source. location near either the. nose or the. tail of the heliosphere. For the.specifk geometry involved, the directions of the nose and tail turn out to be nearly independent of the distance to the source (less than one degree variation for distances greater than about 100 AU). The variations in the observed source directions is probably related to the fact that the 3.11kHz channel is responding to the upward drifting narrow-band features (see Figure 1), which are clearly evolving during the course of the event.

Relationship to The Great Forbush Decrease of 1991

Only one previous heliospheric radio emission event has been observed with intensities comparable to the 1992-93 event. This event occurred in 1983-84, and was first described by Kurth et al. (7). Five other extremely weak events have been observed between these two major events (8), one in late 1985, one in 1989, and three in 1990-91. Several investigators have searched for unusual effects in the solar wind that might trigger these radio emissions. For example, McNutt (9) first suggested that a high-speed solar wind stream could trigger the radio emission when it reached the terminal shock. This idea was explored further by Grzedzielski and Lazarus (10), who identified a series of dynamic pressure increases in the solar wind that they believed were responsible for the 19 S3-84, 1985, and 1989 events. Despite the possible merit of these suggestions, the cause- effect relationship was not convincingly demonstrated, and other sources continued to be considered. For an overview of the situation prior to the 1992-93 event, see Kurth (8).

Since heliospheric radio emission events comparable to the 1992? -93 event are extremely rare, one would expect that the solar wind trigger would also be an unusual event. During the period prior to the. 1992-93 radio emission event, there is one event, the great Forbush decrease of 1991, that fits this requirement. For many years it has been known that the Sun occasionally ejects an energetic burst of gas called a coronal mass ejection (1 1). The ejection is often associated with a series of solar flares and produces an interplanetary shock wave. that moves outward from the Sun at high speed, up to 1000 km/s. The shock wave is typically followed by a turbulent high-speed stream of plasma. As the shock propagates outward through the heliosphere, the turbulent magnetic fields embedded in the }Iiph-speed stream inhibit the entry of cosmic rays, causing a temporary decrease in the cosmic ray intensity. This effect is called a Forbush decrease (12).

1 Duringthe period from May ?5 to June 15, 1991, a total of six major solar flares occurred (13). This sequence of intense solar flare. activity produced a strong interplanetary shock and one of the largest For bush decreases ever observed. The main features of this event were first discussed by Van Allen and Fillius (14), and Webber and Lockwood (1 S). The time sequence of events is illustrated in Figure 4, which has been adapted from data in the above reports. The top panel shows the counting rate from the Deep River neutron monitor, which records the cosmic ray intensity at the Earth. Shortly after the onset of the period of intense solar activity, indicated by the small crosshatched region at the top of the plot, a large (~ 30%) Forbush decrease develops in the. neutron monitor data. This decrease is the deepest depression ever observed by a neutron monitor in over thirty years of observations. The next four panels show the cosmic ray intensities from Pioneer 10 and 11, at 53 and 34 AU, and from Voyagers 1 and 2, at 46 and 35 AU. As the shocks generated by the solar activity propagate outward from the Sun, they are believed to coalesce into a single shock followed by a region of turbulent high-speed plasma called a merged intro action region (16). As the disturbed plasma sweeps over the Pioneer and Voyager

spacecraft, roughly three to four months after the flare activity, strong decreases occur in the cosmic ray intensities, first at Pioneer 11, then at Voyagers 2 and 1, and finally at Pioneer 10. The shock itself was also detected, first by the magnetometer on Pioneer 11 (17), then by the plasma instrument on Voyager ? (5), and finally by the plasma wave instrument on Voyager 1 (14). These shocks are indicated by arrows in Figure 4. From the timing of the various events, Van Allen and Fillius estimate that the. average. propagation speed is 820 km/s. Webber and Lockwood give propagation speeds ranging from 600 to 800 km/s. The overall propagation time, from the onset of the solar activity on day 145, 1991, to the onset of the radio emission event on day 188, 1992, is 408 days or 1.1? years.

Although the 1992-93 radio mission event and the interplanetary shock associated with the 1991 Forbush decrease are both extraordinary events, one case does not prove a cause-effect relationship. However, upon reexamining the 1983-84 heliospheric radio emission event, which started on day 242, 1983, a very large (21%) Forbush decrease was found a little over one year earlier, on day 195, 1982. For a discussion of this event, see Van Allen and Randall, and Webber et al. (18). The time interval between the day 195, 1982, Forbush event and the onset of the 1983-84 radio emission is 412 days, or 1.13 years, almost exactly the same as the 1992-93 radio emission event. Also, the propagation speeds, 810 and 850 km/s, given by Van Allen and Randall, and Webber et al., are almost exactly the same as the speed given by Van Allen and Fillius (14) for the 1991 Forbush event. Thus, the two strong heliospheric radio emission events observed by Voyager both appear to have been triggered by interplanetary shocks with large. Forbush decreases.

INTERPRETATION OF THE RADIO EMISSION SPECTRUM

The frequency-time spectrum of the 1992-93 radio emission event is very' complex. To interpret this spectrum, we. assume that the radio mission is produced by an interplanetary shock, and that the. mission is generated at the plasma frequency, f_p, and/or its harmonic, $2f_p$. The generation of radio emission at f_p and $2f_p$ by an interplanetary shock is well known and is the basic mechanism involved in the generation of Type 11 solar radio bursts (19). It is also the only mechanism that has been previously considered for explaining the heliospheric radio emissions (20).

Three boundaries must be considered as the interplanetary shock propagates outward from the Sun: the terminal shock, the heliopause, and the bow shock. The geometry involved is illustrated in Figure S. Most previous heliospheric radio emission models have. focused on the terminal shock as the source region. However, in this case the radio emission cannot be. generated at the terminal shock, or in the region between the terminal shock and the heliopause. 'l'he. reason is that the electron plasma frequency is too low. Given the observed propagation speed of 600 to 800 km/s and travel time of -1.1 years, the terminal shock would have to be located at a distance of 140 to 186 AU. At this great distance the electron plasma frequency, which varies as 1/1<, would be only about 100 to 150 Hz. Since the electron plasma frequency can only increase by a factor of two at a shock, and since the highest frequency that can be generated is twice the electron plasma frequency, it would be impossible to generate the observed frequencies.

At the heliopause the situation is much better. The plasma density at the heliopause is controlled by pressure balance. Since the. temperature on the interstellar side of the heliopause is expected to be

much colder than cm the solar wind side, the electron plasma frequency can increase by a large factor at the heliopause, to a value that is comparable to the plasma frequency in the interstellar medium. From numerical simulations (21) and various physical arguments, the plasma frequency profile in the vicinity of the heliopause is believed to be as shown in Figure 6. The plasma frequency immediately inside of the bow shock depends on the strength of the bow shock, and cannot be more than twice the plasma frequency in the interstellar medium. Remote sensing measurements (?2) suggest that the electron density in the local interstellar medium is about 0.03 to 0.1 cm^{-3}, which corn esponds to a plasma frequency of about 1.6 to 2.8 kHz. These plasma frequencies are in the same general range as the observed radio emission frequencies, and are therefore consistent with generat ion in the. vicinity of the heliopause. Just why the radio emission should turn on as the interplanetary shock encounters the heliopause is unknown. Most likely the onset is related to the much lower temperatures of the. interstellar medium, which would reduce the Landau damping, thereby possibly causing higher radio emission intensities.

Once the interplanetary shock has crossed the heliopause, the mission frequency depends on the plasma frequency encountered by the shock as it propagates through the post-heliopause plasma. Numerical simulations show that there is a pile. up of plasma around the nose. of the. heliosphere (21). A cut along the line A-B-C in Figure 5 would therefore be expected to give a peak in the electron plasma frequency profile, as shown by the curve A-B-C in Figure 6. A shock propagating through this region would then give an emission frequency that increases with increasing time, as indicated by the curve labeled A-B in the top right-hard corner of Figure 6. The rising emission frequency is believed 10 account for the upward drifting narrow-band emissions evident in Figure 1. This interpretation also predicts a source near the nose of the heliopause, which is consistent with the direction finding measurements described earlier. It is not clear whether the radiation is produced at f_p, $2f_p$, or at both.

For the segment of the shock front propagating through the flanks of the heliopause, as along line A-B′-C in Figure 5, the mission frequency should be nearly constant. Radiation from this region is believed to account for the main emission band in Figure 1 which is nearly constant at a frequency of about 2.o kHz. In the simplest interpretation the radiation would not be trapped in the heliospheric cavity. However, the issue of trapping depends sensitively on the details of the plasma frequency profile (which is poorly known), and the exact point where the emission turns on. It is possible that some or all of the radiation generated in the immediate vicinity of the heliopause could be. trapped in the heliospheric cavity. The absence of detectable roll modulation in the 1.78 kHz channel does not rule out trapping in this frequency range. We are also not completely certain how to interpret the enhancement at about 2.7 kHz. One possibility is that the main band at 2.0 kHz is caused by emission at the fundamental, f_p, and the enhancement around 2.7 kHz is caused by emission at the harmonic, $2f_p$. An obvious problem with this interpretation is that the ratio of the frequency of the upper band to the frequency of the lower band is only 1.35, which dots not indicate a harmonic relationship. Similar, though smaller, discrepancies also occur for Type 11 solar radio bursts (19). Another possibility is that the 2.0 and 2.7 kHz components are emitted from two regions that have different plasma densities, hence different plasma frequencies. Without more detailed information on the plasma density distribution, it is difficult to (distinguish between such interpretations.

Finally, we consider the low frequency cutoff of the spectrum at 1.8 kHz. 'l'here arc two possible interpretations: first, that it is a propagation cutoff at the plasma frequency; and second, that it is a characteristic emission frequency (either f_p or $2f_p$) in the source. If it is a propagation cutoff then the most likely possibility is that it corresponds to the plasma frequency in the post-heliopause region along tile. flanks anti downstream tail region, where the plasma density is near the interstellar value. in this case the electron density in the interstellar medium would be about 0.04 cm^{-3}. If the cutoff is a source. effect

then the plasma density in the source would be 0.04 cm^{-3} if the emission is at the fundamental, or 0.01 cm^{-1} if it is at the harmonic.

Distance to the Heliopause

The distance to the heliopause can be computed from the propagation speed of the interplanetary shock and from the travel time from the Sun to the heliopause. The difficulty with this calculation is that the shock almost certainly slows down after passing through the terminal shock. Since the propagation speed in the region beyond the terminal shock is unknown, certain simplifying assumptions must be made. As a simple model we assume that the shock propagates with a constant speed, V_1, inside of the terminal shock, and with a slower constant speed, V_2, outside of the terminal shock. To take into account the unknown speed V_2, we introduce a speed parameter, $\alpha = V_2/V_1$, which is the ratio of the speed after the terminal shock, to the speed before the terminal shock. Since the distance to the terminal shock is also unknown, we also introduce a distance. parameter, $\delta = R_T/R_H$, which is the ratio of the distance to the terminal shock, k_T, to the distance to the heliopause, R_H. Using these two parameters, it can be shown that the. distance to the heliopause is given by

$$R_H = V_1 T \left[\frac{\alpha}{1-(1-\alpha)\delta}\right]$$

where T is the total travel time from the Sun to the heliopause. For an initial estimate we use T =- 1.1 year and V_1 = 600 to 800 km/s. These values arc consistent with both the 1983-84 and 1992-93 events. For the distance parameter δ, numerical simulations (21) suggest an average value of about 0.75, with a range from about 0.7 to 0.8. For the shock speed parameter α, numerical simulations (23) suggest a nominal value of about 0.7, with a range from 0.6 to 0.8. 'l'able 1 summarizes the distances to the heliopause using various combinations of these parameters. These calculations place the distance to the

heliopause in the range from about 116 to 177 AU. By using numerical simulations it should be possible to greatly improve the accuracy of these estimates.

TABLE CAPTIONS

Table 1. The distance to the heliopause as a function of the parameter CY, which is the ratio of the interplanetary shock speed beyond the terminal shock, V_2, to the speed inside the terminal shock, V_1, and the parameter δ, which is the ratio of the distance to the terminal shock, R_T, to the distance to the heliopause, R_H.

V_1 = 800 km/s

		$\alpha = V_2/V_1$		
		0.6	0.7	0.8
$\delta = R_T/R_H$	0.80	164 AU	172 AU	177 AU
	0.75	160 AU	168 AU	175 AU
	0.70	155 AU	165 AU	173 AU

V_1 = 600 km/s

		$\alpha = V_2/V_1$		
		0.6	0.7	0.8
$\delta = R_T/R_H$	0.80	123 AU	129 AU	133 AU
	0.75	120 AU	126 AU	131 AU
	0.70	116 AU	124 AU	140 AU

TABLE I

REFERENCES AND NOTES

1. E. N. Parker, *Interplanetary Dynamical Processes* (Interscience, New York, NY, 1963)
2. W.]. Ax ford, in Physics *of the Outer Heliosphere*, S. Grzedzielski and D.E. Page, Eds. (Pergamon Press, Oxford, 1990), pp. 7-15.
3. S. "I'. Suess, *Reviews of Geophys.* 28, 97 (1990).
4. F.L. Scarf and D.A. Gurnett, *Space Sci. Rev.* **21**, 289 (1977).
5. J. Belcher, personal communication (1993).
6. A. Czechowski and S. Grzedzielski, *Nature*, **344**, 640 (1990).
7. W.S. Kurth, D.A. Gurnett, F.L. Scarf, R.L. Poynter, *Nature* **312**, 27 (1984).
8. -.. —.. , *Geophys. Res. Lett.* 14, 49 (1987); W.S. Kurth and D.A. Gurnett, *ibid.* 18, 1801 (1991); W.S. Kurth, *Adv. Space* Res., in press (1993).
9. R.L. McNutt, *Geophys. Res. Lett.* **1** *S, 1307* (1988).
10. S. Grzedzielski and A.J. I azarus, *J. Geophys. Res.* 98, 5551 (1993).
11. J .D. Gosling, et al., *J. Geophys. Res.* 79, 4581 (1974); S.W. Kahler, *Ann.* Rev. *Astron. Astrophys.* **30**, 113 (1992); J .D. Gosling, The Solar Flare M yth, in press, *J. Geophys.* Res. (1993).
12. S.E. Forbush, *Phys. Rev.* S1, 1108 (193-/).
13. *Solar-Geophysical Data*, various issues, NOAA, Boulder (1991, 1992).
14. J.A. Van Allen and R.W. Fillius, *Geophys. Res. Lett.* 19, 1423 (1992).
15. W .R. Webber and J .A. Lockwood, *J. Geophys. Res.* 98, 7821 (1993); see also F.B. McDonald et al., Proceedings of the 23rd Internat. Cosmic Ray Conf., Calgary, 19-30 July (1993).

16. 1,.1:. Burlaga et al., *J. Geophys. Res. 89, 6579 (1984);* L.F. Burlaga, F.B. McDonald, N.F. Ness, A.J. Lazarus, *ibid. 96, 3780 (1991).*

17. D. Winterhalter, E.J. Smith, L.W. Klein, *EOS Trans. AGU* **73**, *237 (1992).*

18. J.A. Van Allen and B.A. Randall, *J. Geophys. Res. 90, 1399 (1985); W.* R. Webber, J. A. Lockwood, and J. R. Jokipii, *J. Geophys. Res.* 91, 4103 (1986).

19. G.B. Nelson and D.B. Mel rose, in *Solar Radiophysics*, D.J. McLean and N.R. Lebrum, Eds. (Cambridge Univ. Press, Cambridge, 1985), pp. 333-3S9.

20. W.M. Macek, I.H. Cairns, W.S. Kurth, D.A. Gurnett, *Geophys. Res. Lett.* 18, 357 (1991); I.H. Cairns and D.A. Gurnett, *J. Geophys. Res.* 97, 623S 91992); I.H. Cairns, W.S. Kurth, D.A. Gurnett, *ibid. 97, 6245 (1992).*

21. V. B. Baranov, *Space Sci. Rev.* S2, 89 (1990); V .B. Baranov and Yu. G. Malama, unpublished report, 1992; R.S. Steinolfson, V.J. Pine, 'l'. Holzer, *Geophys. Res. Lett.*, submitted (1993).

22. A.F. Davidsen, *Science* 2S9, 32-/ (1993); R. Lallement, J.-1.,. Bertaux, J.T. Clark, *ibid.* 260, 1095 (1 **993).**

23. R. **S.** Steinolfson, personal communication (1993).

24. J. M. Ajello, A. I. Stewart, (i. E. Thomas, A. Garps, *Ap. J.* 317, 964 (1987).

25. We thank the Voyager team at the Jet Propulsion Laboratory (JPL) for their valuable support. We are especially grateful to E. Storm, E. Franzgrote, and S. Linick for scheduling increased wideband coverage during this event, and to C. Avis and N. Toy for timely and efficient production of the experiment data records. At Goddard Space Flight Center, we thank R. Lepping for his help in determining the spacecraft attitude during the roll maneuver, and at the University of Iowa, we thank J.A. Van Allen for numerous useful discussions, and L. Granroth, J. Cook-Granroth, and T. Barnett-Fisher for their efforts in processing the data. The research at the University of Iowa was supported by NASA through contract 959193 with JPL.

FIGURE CAPTIONS

Figure 1. Frequency-time spectrograms of the **1992-93** heliospheric radio emission event. The top pad is from Voyager 1, and the bottom panel is from Voyager ?. The color indicates the electric field intensity, with red being the most intense and blue being the least intense.

Figure 2. A plot of the electric field intensity in the 3.11 kHz channel during a ten turn roll maneuver on day 220, 1992.. A clear roll modulation signal can be seen. The phase of the roll modulation gives the direction to the source.

Figure 3 Source directions at 3.11 kHz determined from roll maneuvers on days 220 and 311, 1992., and on day 36, 1993. The view is from the. spacecraft looking along the roll axis (β = -33.7°, λ = 63.7°) toward the Earth. The horizontal (reference) direction has been taken to be the direction of the Sun's motion with respect to the nearby interstellar medium, β = **S.O**° and λ = 254°, as given by Ajello (24).

Figure 4. Cosmic ray counting rates at Earth, Pioneers 10 and 11 (53 and 34 AU), and Voyagers 1 and 2 (46 and 35 AU). The sharp decreases in the cosmic ray counting rates are produced by an outward propagating interplanetary shock generated by a series of large solar flares in late May and early June, 1991. Illustration adapted from Van Allen and Fillius (14), and Webber and Lockwood (15).

Figure 5. A sketch of the heliosphere and its anticipated boundaries. The heliopause is the boundary between the solar wind and the interstellar plasma. Since. the solar wind flowing out from the Sun is supersonic, a standing shock, called the terminal shock, is expected to form in the solar wind flow somewhat inside of the heliopause. A second

standing shock, called the bow shock, is expected to form in the interstellar plasma flow upstream of the heliosphere. "I"he outward propagating interplanetary shock produced by the solar activity in late May and early June, 1991, is indicated by circle with outward directed arrows. The approximate positions of Pioneers 10 and 11 (1'10 and PI 1) and Voyagers 1 and 2 (V 1 and V2) are indicated by the dots,

Figure 6. A representative electron plasma frequency (f_p) profile through the terminal shock, the heliopause, and the. bow shock, "I'he peak in the profile along A-B-C (see also Figure 6) is caused by the "pile up" of plasma near the nose of the heliosphere, and is believed to account for the upward drifting narrowband emissions in Figure 1. 'I'he nearly constant frequency emission at - 2..0 kHz is believed to be p~-educed from the flanks of the heliosphere, along A-B'-C, where. the plasma frequency is nearly constant, The 1.8 kHz cutoff would then be indicative of the plasma frequency in this region.

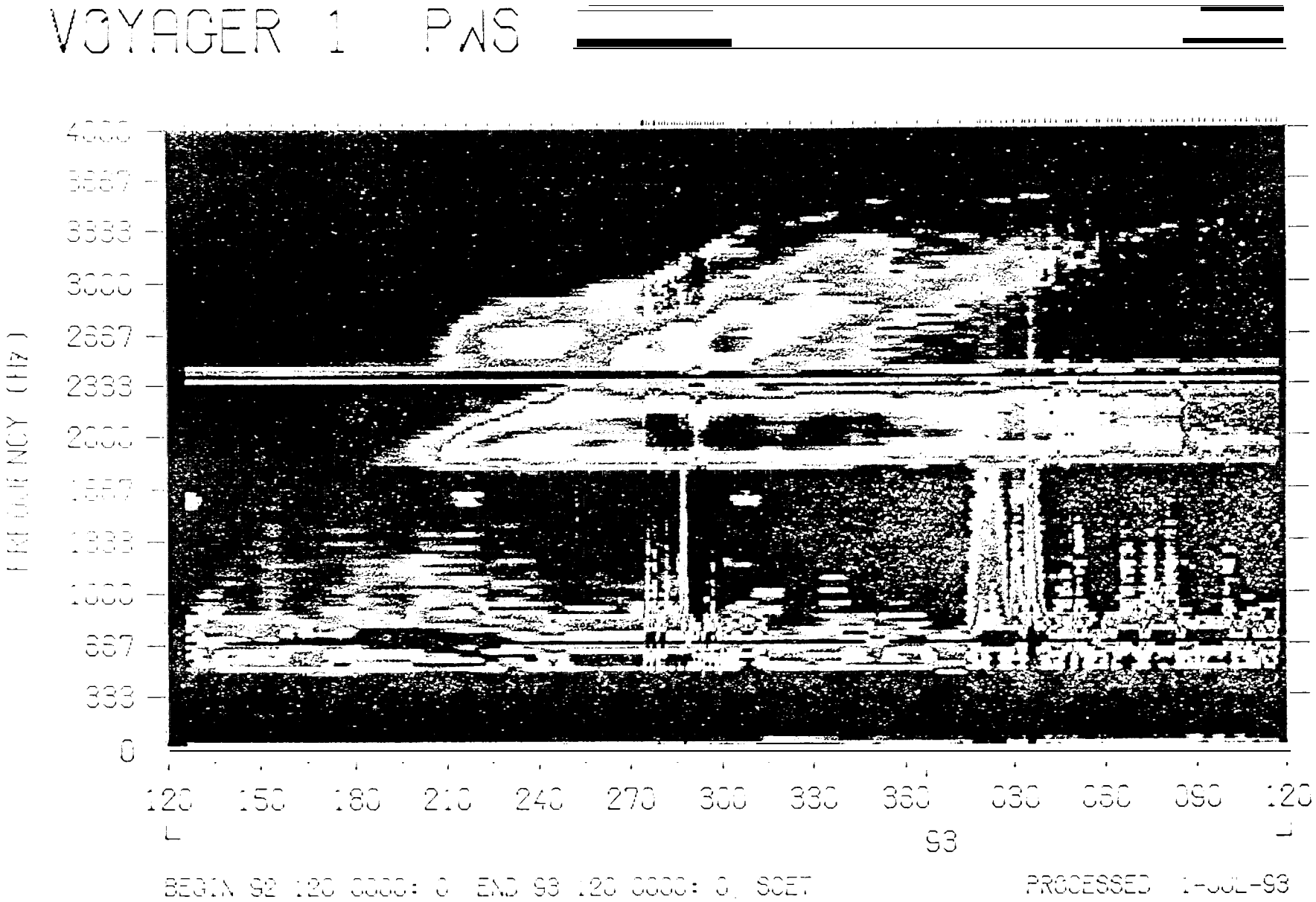
VOYAGER 1 PWS
4000
3667
3333
3000
2667
2333
2000
1667
1333
1000
667
333
0
FREQUENCY (Hz)
120
150
180
210
240
270
300
330
360
030
060
090
120
93
BEGIN 92 120 0000: 0 END 93 120 0000: 0 SCET
PROCESSED 1-JUL-93

Figure 1A

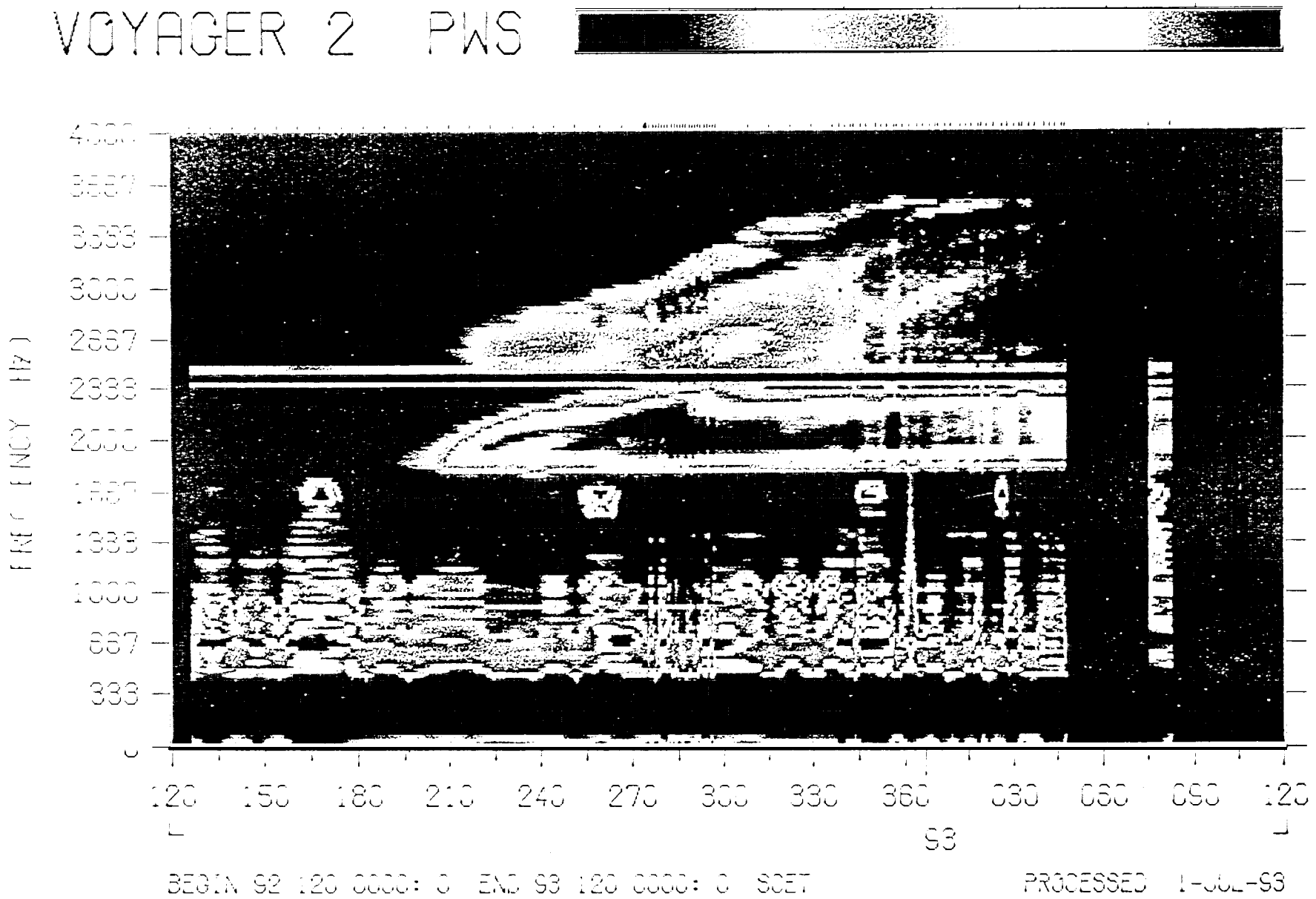
VOYAGER 2 PWS
333
0
120
150
180
210
240
270
300
330
360
030
060
090
120
S3
BEGIN S2 120 0000: 0 END S3 120 0000: 0 SCET
PROCESSED 1-JUL-93

Figure 1.3

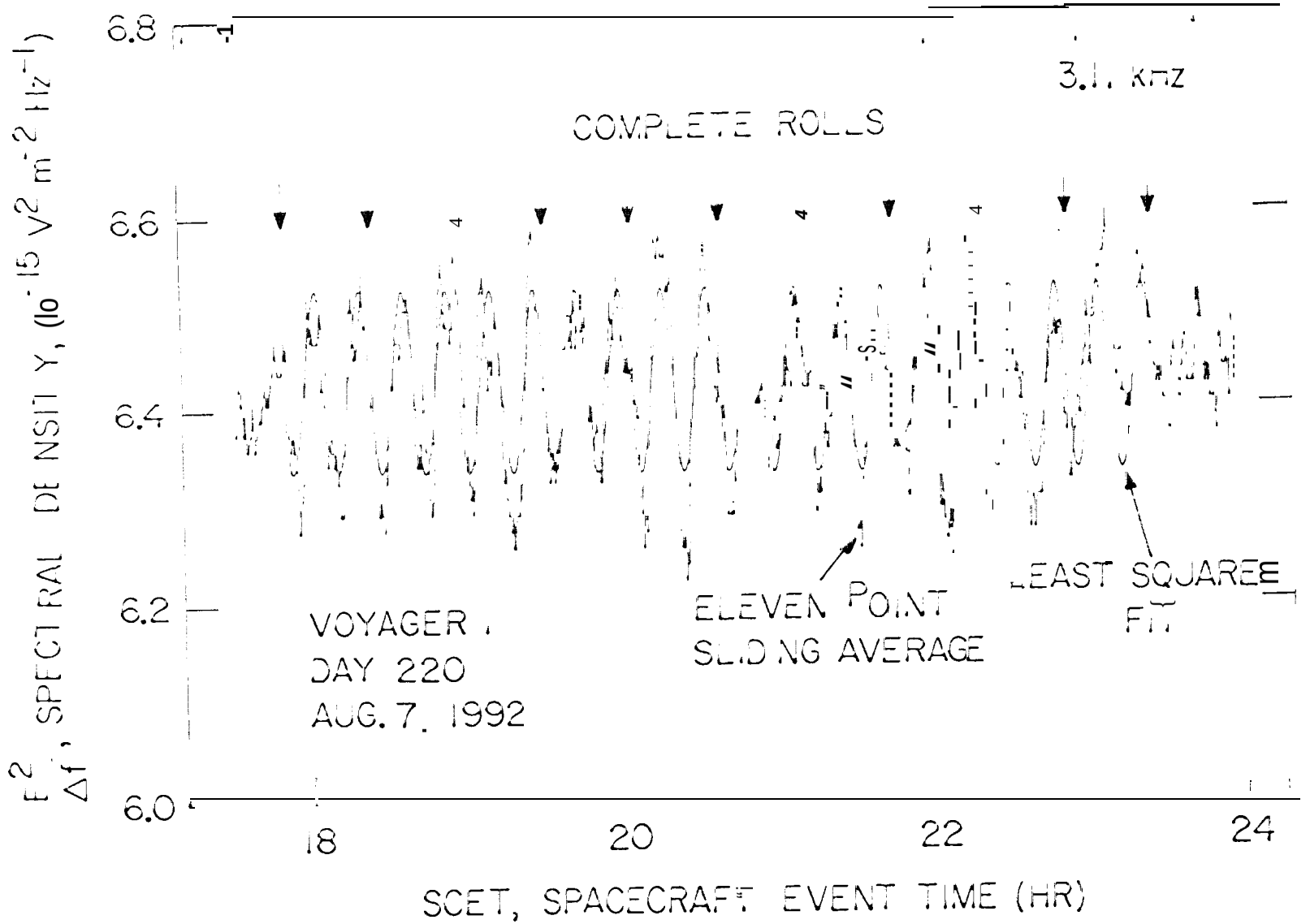
3.1 KHZ
COMPLETE ROLLS
6.8
6.6
6.4
6.2
6.0
$E^2/\Delta f$, SPECTRAL DENSITY, (10^{-15} V^2 m^{-2} Hz^{-1})
VOYAGER 1
DAY 220
AUG. 7, 1992
ELEVEN POINT
SLIDING AVERAGE
LEAST SQUARES
FIT
18
20
22
24
SCET, SPACECRAFT EVENT TIME (HR)

Figure 2

A-693-277

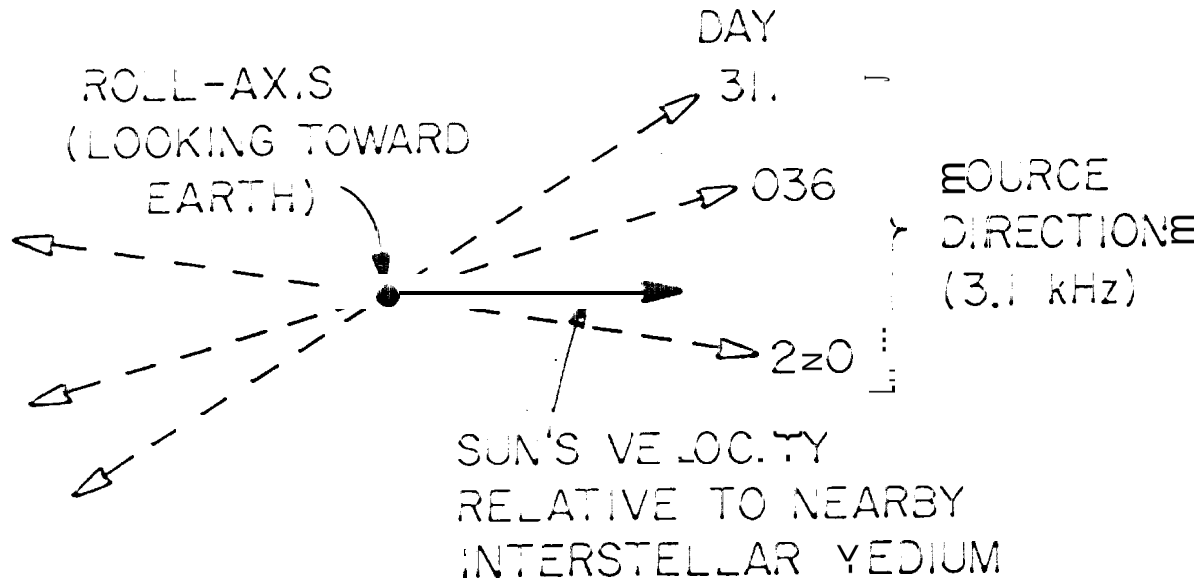

Figure 3

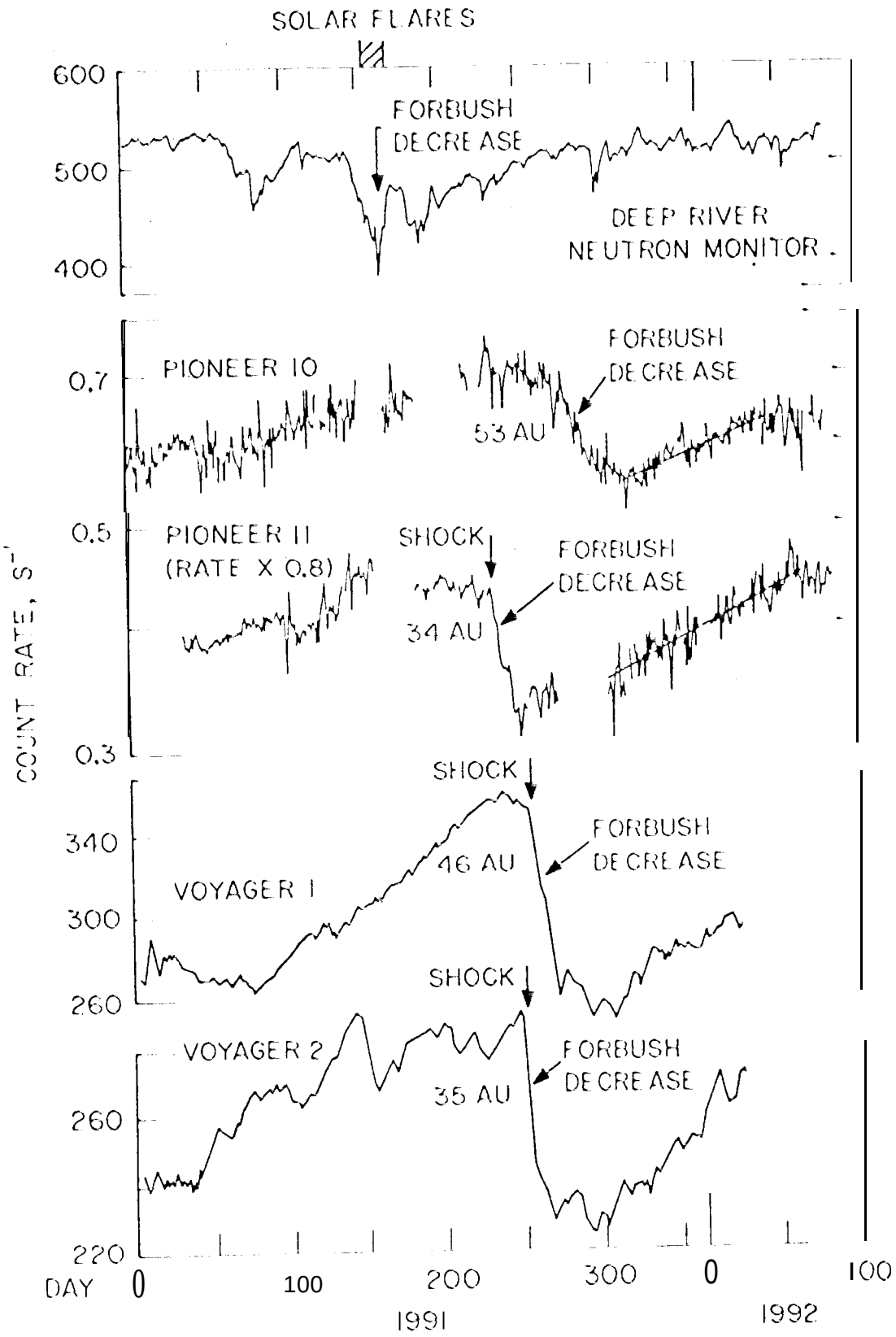
SOLAR FLARES
600
500
400
FORBUSH
DECREASE
DEEP RIVER
NEUTRON MONITOR
0.7
PIONEER 10
FORBUSH
DECREASE
53 AU
0.5
PIONEER 11
(RATE X 0.8)
SHOCK
FORBUSH
DECREASE
34 AU
0.3
COUNT RATE, S⁻¹
SHOCK
340
FORBUSH
DECREASE
46 AU
VOYAGER 1
300
SHOCK
260
VOYAGER 2
FORBUSH
DECREASE
35 AU
260
220
DAY
0
100
200
300
0
100
1991
1992

Figure 4

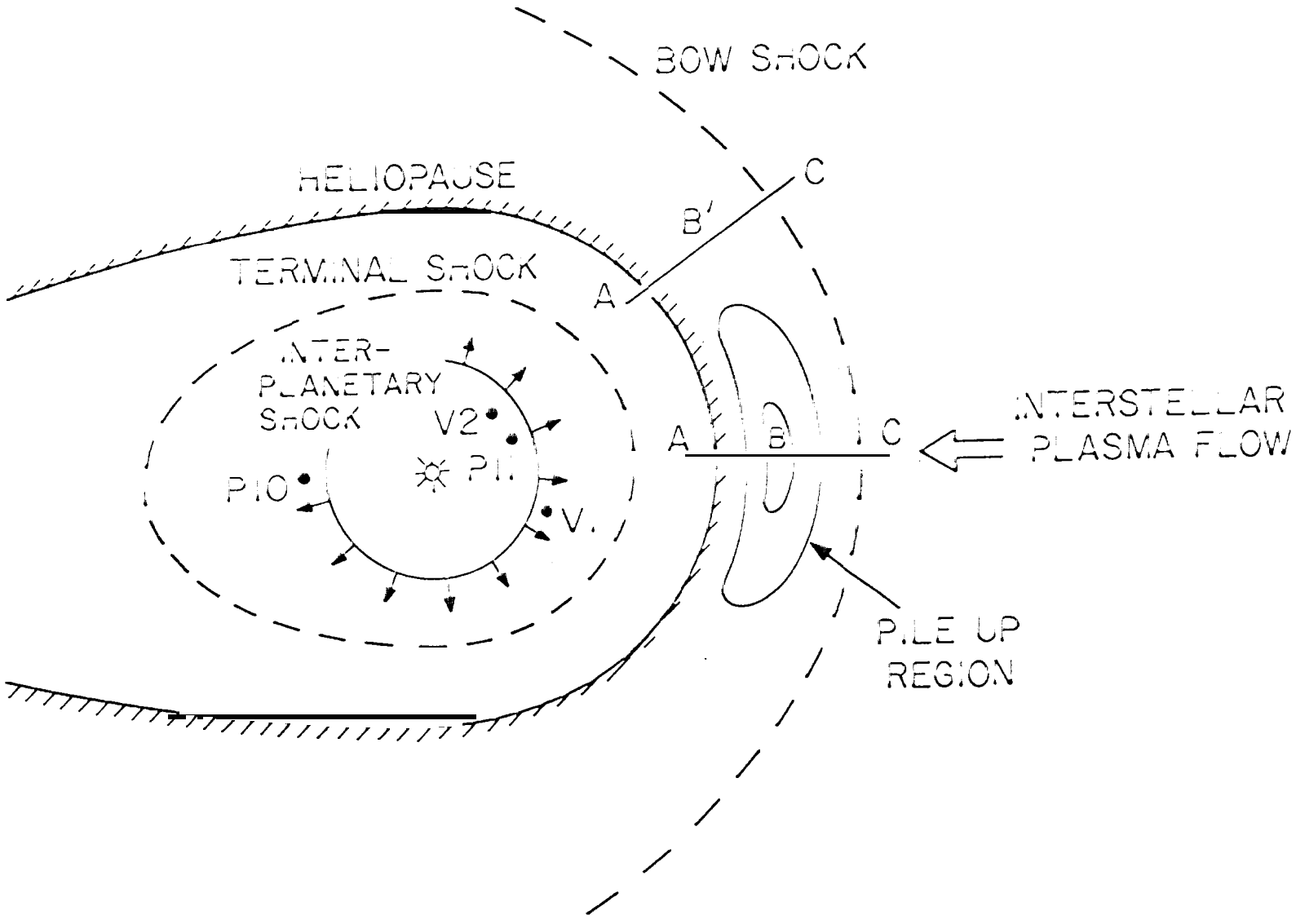
BOW SHOCK
HELIOPAUSE
C
B'
TERMINAL SHOCK
A
INTER-
PLANETARY
SHOCK
V2
P.O
P.I.
V.
A
B
C
INTERSTELLAR
PLASMA FLOW
PILE UP
REGION

Figure 5

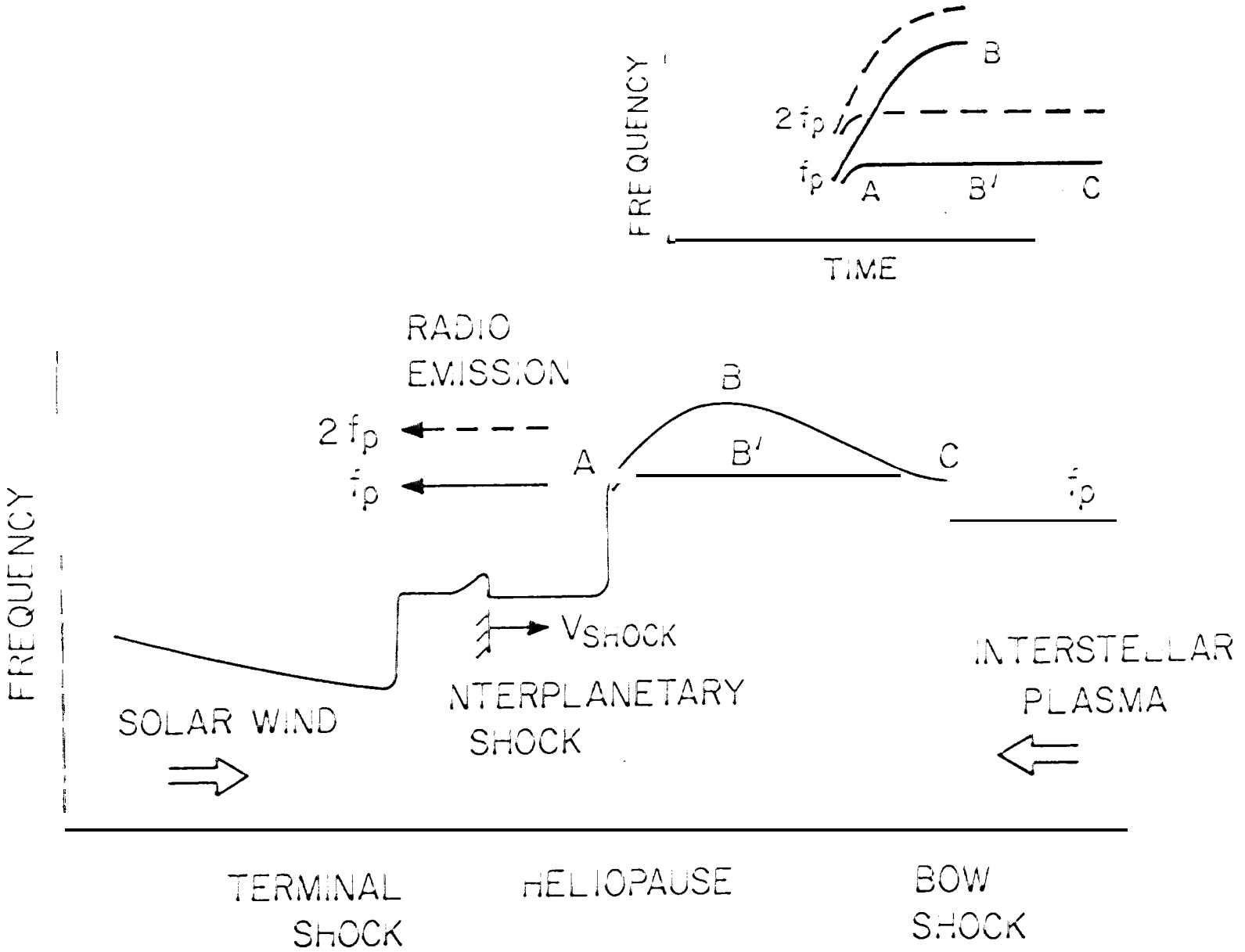
FREQUENCY
B
2 fp
fp
A
B'
C
TIME
RADIO
EMISSION
2 fp
fp
A
B
B'
C
fp
FREQUENCY
VSHOCK
SOLAR WIND
NTERPLANETARY
SHOCK
INTERSTELLAR
PLASMA
TERMINAL
SHOCK
HELIOPAUSE
BOW
SHOCK

Figure 6